FUDMA Journal of Sciences (FJS)
ISSN online: 2616-1370
ISSN print: 2645 - 2944
Vol. 10 No. 16, June, 2026, pp 628 – 634
DOI: https://doi.org/10.33003/fjs-2026-1016-5925

Dynamical Analysis and Spatial Distribution of Field Strength Variability across Nineteen Locations in Nigeria: A Nonlinear Approach for Communication Planning

Jamila Abdullahi Bichi

Department of Physics, Bayero University Kano, Kano State, Nigeria.

*Corresponding authors' email: jabichi.phy@buk.edu.ng Phone: +2348039229027

ABSTRACT
Field Strength Variability (FSV) is an important atmospheric propagation parameter that influences terrestrial and satellite communication performance through signal fading, ducting and multipath effects. This study presents a dynamical analysis and spatial distribution of FSV across nineteen locations in Nigeria using a nonlinear approach based on the Hurst Exponent (HE) and Lyapunov Exponent (LE). The selected locations represent the Sahel/Sudan Savanna, Guinea Savanna and Rainforest/Coastal climatic zones. Daily meteorological data obtained from the NASA Modern-Era Retrospective Analysis for Research and Applications, Version 2 (MERRA-2), covering 1982–2022, were used to compute radio refractivity and derive FSV. The spatial analysis revealed a clear north-to-south variation, with higher regional mean FSV values in the Sahel/Sudan Savanna (8.47 dB), decreasing through the Guinea Savanna (7.23 dB) to the Rainforest/Coastal region (4.81 dB). The nonlinear dynamical analysis showed that HE values ranged from 0.2544 to 0.3850, with all values below 0.5, indicating predominantly anti-persistent behaviour. The LE analysis revealed distinct regional dynamics, with positive values predominantly occurring in the Sahel/Sudan and Guinea Savanna regions, indicating sensitive dependence on initial conditions and chaotic behaviour, whereas predominantly negative values in the Rainforest/Coastal region indicated relatively more stable dynamics. The findings demonstrate that both the magnitude and nonlinear characteristics of FSV are strongly influenced by spatial and climatic variability across Nigeria. This study provides insight into the spatial distribution and dynamical behaviour of FSV in tropical environments and offers useful information for radio propagation assessment, communication planning and the development of region specific propagation strategies. Such strategies may support improved communication link reliability by accounting for differences in atmospheric dynamics across Nigeria's contrasting climatic regions.

Received: 28 Aug. 2026
Accepted: 01 Sep. 2026
Published: 09 Sep. 2026

Keywords: Field Strength Variability; Hurst Exponent; Lyapunov Exponent; Nonlinear Dynamics; Radio Refractivity

INTRODUCTION

Field Strength Variability (FSV) is an important parameter in assessing terrestrial and satellite communication performance because atmospheric fluctuations can cause signal fading, anomalous propagation, multipath effects and variations in link availability (Ajayi *et al.*, 1984; ITU-R, 2023). These effects are particularly relevant in tropical regions such as Nigeria, where atmospheric conditions are strongly influenced by temperature, humidity, precipitation, convection, and seasonal variations. Variations in these atmospheric parameters modify radio refractivity and its vertical gradients, thereby affecting tropospheric propagation and the stability of radio signals (Adediji *et al.*, 2008; ITU-R, 2019). Recent studies in Nigeria have continued to demonstrate the importance of atmospheric variables in determining radio refractivity and propagation conditions (Akpootu *et al.*, 2024; Ashidi, 2024).

Despite the importance of FSV in communication system planning, its temporal dynamics and nonlinear characteristics remain relatively underexplored in Nigeria and the wider West African region. Previous studies have mainly focused on the spatial and seasonal variability of FSV and radio refractivity using conventional statistical approaches and empirical propagation models. For example, Tanko *et al.* (2022) investigated the spatial and seasonal variation of FSV across 61 locations in Nigeria and reported higher FSV during the dry season than during the wet season. More recently, Ibrahim *et al.* (2024) examined the variability of tropospheric radio refractivity and field strength over Enugu and demonstrated the influence of atmospheric conditions on FSV. Although such studies provide valuable information on the climatological behaviour of FSV, they do not fully describe its nonlinear temporal structure, memory characteristics or dynamical stability.

Atmospheric variables influencing FSV interact over multiple temporal and spatial scales, producing complex time dependent behaviour. Consequently, nonlinear dynamical approaches can provide additional information that may not be adequately captured by conventional statistical techniques. In particular, the Hurst exponent (H) and Lyapunov exponent (LE) provide complementary measures for characterizing the temporal dynamics of atmospheric time series. The Hurst exponent describes the long-term dependence or memory of a time series. Values of $H > 0.5$, $H = 0.5$, and $H < 0.5$ are generally associated with persistent, random, and anti-persistent behaviour, respectively (Hurst, 1951; Kantelhardt *et al.*, 2002). The Lyapunov exponent measures the average rate of divergence or convergence of initially close trajectories in a dynamical system. A positive largest Lyapunov exponent indicates sensitive dependence on initial conditions and is commonly associated with chaotic behaviour, whereas a negative value indicates convergence and greater dynamical stability (Wolf *et al.,* 1985; Rosenstein *et al.*, 1993).

Nonlinear methods have been applied in atmospheric and geophysical studies to investigate the temporal dynamics and predictability of variables such as rainfall, temperature, and radio refractivity (Echi *et al.*, 2015; Fawupe *et al.*, 2016; Rasoul *et al.*, 2014). Recent work has also demonstrated the usefulness of nonlinear indicators for examining the temporal variability and predictability of radio refractivity in Nigeria. Bichi *et al.* (2025) applied recurrence analysis, the Hurst exponent, and the Lyapunov exponent to radio refractivity time series across selected Nigerian locations and reported distinct nonlinear characteristics associated with climatic conditions. These findings suggest that nonlinear methods can provide useful insight into the dynamical behaviour of atmospheric propagation parameters.

However, a comprehensive assessment of the nonlinear characteristics of FSV across the major climatic environments of Nigeria remains limited. In particular, the spatial variation of FSV dynamics across the Sahel/Sudan Savanna, Guinea Savanna, Rainforest, and Coastal regions has not been adequately examined using complementary Hurst and Lyapunov exponent approaches. Addressing this gap is important because differences in atmospheric moisture, temperature, pressure, and seasonal behaviour across Nigeria can produce distinct FSV characteristics and, consequently, different implications for radio propagation and communication system planning.

This study therefore investigates the nonlinear characteristics of FSV across nineteen locations representing the major climatic regions of Nigeria using long-term atmospheric data from the NASA Modern-Era Retrospective Analysis for Research and Applications, Version 2 (MERRA-2), covering 1982–2022. FSV time series derived from computed radio refractivity are analysed using the Hurst and Lyapunov exponents to assess memory characteristics, dynamical stability, and predictability. The study further compares the nonlinear behaviour of FSV across the different climatic regions to identify spatial patterns associated with atmospheric variability. The findings provide a nonlinear perspective on FSV dynamics and contribute to improved understanding of atmospheric influences on radio propagation across Nigeria, with potential applications in propagation modelling, communication system planning and radio link reliability assessment.

MATERIALS AND METHODS

Study Area

The study covered nineteen selected locations representing the major climatic zones of Nigeria, namely the Sahelian, Sudanian, Guinea Savanna, Rainforest and Coastal zones. The selected locations were Sokoto, Katsina, Kano, Yobe, Borno, Niger, Taraba, Plateau, Benue, Federal Capital Territory (FCT), Edo, Ekiti, Ebonyi, Anambra, Enugu, Lagos, Akwa Ibom, Rivers, and Bayelsa. These locations provide a broad geographical representation of the contrasting atmospheric and climatic conditions across northern, central and southern Nigeria. The geographical coordinates of the selected locations are presented in Table 1.

Table 1: Geographical coordinates of the selected locations (NASA (2000), as reported by Bichi *et al.* (2026)

S/No.	Location	Latitude (°N)	Longitude (°E)	Altitude (m)
1	Sokoto	13.0501	5.2251	307
2	Katsina	13.0510	7.5900	508
3	Kano	12.0007	8.5266	546
4	Yobe (Damaturu)	12.8771	10.4516	300
5	Borno (Maiduguri)	11.8251	13.1024	360
6	Niger (Minna)	9.6051	6.5463	311
7	Taraba (Jalingo)	8.9034	11.3542	400
8	Plateau (Jos)	9.8630	8.8810	1,208
9	Benue (Makurdi)	7.7100	8.6260	104
10	FCT (Abuja)	9.0610	7.4760	360
11	Edo (Benin City)	6.3611	5.6263	200
12	Ekiti (Ado-Ekiti)	7.6463	5.2251	480
13	Ebonyi (Abakaliki)	6.3080	8.1080	117
14	Anambra (Awka)	6.1270	5.7670	103
15	Enugu (Enugu)	6.4490	7.5110	199
16	Lagos (Ikeja)	6.4548	4.4136	5
17	Akwa Ibom (Uyo)	5.0278	7.9336	38
18	Bayelsa (Yenagoa)	4.8121	7.0629	10
19	Rivers (Port Harcourt)	4.9523	6.3066	29

Materials

The computational tools used in this study included a personal computer running Windows 11, MATLAB R2020a, Microsoft Excel, Microsoft Word, and QGIS. MATLAB R2020a was used for data processing, statistical analysis, visualization, nonlinear analysis, and implementation of the machine learning models. Microsoft Excel was used for data organization, tabulation and preliminary data processing. QGIS was used to produce the spatial distribution maps of FSV and the nonlinear indices across the selected locations, while Microsoft Word was used for documentation and preparation of the manuscript.

Data Source and Processing

The meteorological data used in this study were obtained from the Modern-Era Retrospective Analysis for Research and Applications, Version 2 (MERRA-2), developed by the Global Modeling and Assimilation Office (GMAO) of the National Aeronautics and Space Administration (NASA). MERRA-2 is a global atmospheric reanalysis product that combines observations with the Goddard Earth Observing System (GEOS-5) atmospheric model through a data assimilation system to provide long term, spatially and temporally consistent atmospheric datasets (Gelaro *et al.,* 2017).

The MERRA-2 dataset provides hourly two-dimensional meteorological variables at a spatial resolution of 0.5° latitude × 0.625° longitude, corresponding to approximately 50 km in the latitudinal direction. In this study, hourly data covering the period 1982–2022 were obtained for nineteen selected locations representing the Sahel/Sudan Savanna, Guinea Savanna, Rainforest and Coastal climatic zones of Nigeria. NASA documentation confirms that variables such as surface pressure (PS), 2m air temperature (T2M), and 2-m specific humidity (QV2M) are available at hourly intervals in the MERRA-2 dataset.

The meteorological variables extracted from MERRA-2 were 2m air temperature (T2M), surface pressure (PS), and 2m specific humidity (QV2M). Surface pressure represents the atmospheric pressure at the Earth's surface and was used as the pressure input in the radio refractivity calculations. Relative humidity (RH) was derived from the 2m specific humidity. These variables were subsequently used to calculate radio refractivity (RR).

For each selected location, all MERRA-2 grid cells whose centres fell within the corresponding state boundary were identified using their geographical coordinates (latitude and longitude). The values of each meteorological variable from the identified grid cells were spatially averaged at every hourly time step to obtain a representative atmospheric value for the location. The resulting hourly values were then aggregated to daily values for the calculation of radio refractivity. Field Strength Variability (FSV) was subsequently derived from the daily radio refractivity values on a monthly basis. This spatial averaging approach provides representative atmospheric conditions for each study location while reducing the influence of localized variations within individual MERRA-2 grid cells. Table 2 presents the meteorological variables extracted from the MERRA-2 dataset and their applications in the study.

Table 2: Meteorological Variables Extracted from the MERRA-2 Dataset and Their Applications in the Study

S/No	Meteorological Variable	MERRA-2 Parameter Code	Unit	Purpose
1	Air temperature at 2 m	T2M	K	Radio refractivity calculation
2	Surface pressure	PS	Pa (converted to hPa)	Atmospheric pressure input for radio refractivity calculation
3	Relative humidity	Derived	%	Radio refractivity calculation

Data computation

The meteorological data of temperature, pressure and relative humidity were used to compute for the RR and FSV data.

Computation of Radio Refractivity (RR)

The radio refractivity was computed from the extracted meteorological parameters using the standard International Telecommunication Union (ITU-R) recommended formula (ITU-R. 2023);

$$N = 77.6\,\frac{P}{T} + 3.73 \times 10^{5}\,\frac{e}{T^{2}} \quad (1)$$

Where,

N = radio refractivity (N-units), P = surface pressure (hPa), T = absolute temperature (K) and e = water vapour pressure (hPa).

The first term represents the dry component of refractivity, while the second term represents the wet component associated with atmospheric moisture.

The water vapour pressure (e) was determined from the measured relative humidity is related to the relative humidity as (ITU-R, 2023).

$$e = RH \times e_s \quad (2)$$

e_s is the saturated vapor pressure given by (ITU-R 2023);

$$e_s = 6.112\,\exp\left(\frac{17.67T}{T+234.5}\right) \quad (3)$$

Where,

RH is relative humidity (%), e_s = saturated water vapour pressure (hPa), 6.112 (hPa) is the saturated water vapour pressure at 0°C, 17.67 and 243.5°C are empirical constants in the Magnus–Tetens equation for estimating saturated vapour pressure. T = air temperature (°C).

Air temperature obtained from the MERRA-2 parameter T2M was converted from Kelvin to degrees Celsius for the computation of saturation vapour pressure (equation 3) and subsequently converted back to Kelvin for the refractivity calculation (equation 1). Surface pressure obtained from the MERRA-2 parameter PS was converted from pascals (Pa) to hectopascals (hPa) before use in the refractivity equation.

Computation of Field Strength Variability (FSV)

Field Strength Variability (FSV) was estimated from the computed daily radio refractivity values to quantify the temporal fluctuations in atmospheric conditions affecting terrestrial radio wave propagation. Following the approach adopted by Tanko *et al.* (2018, 2022), the maximum and minimum daily radio refractivity values were determined for each month, and the monthly refractivity range was computed as

$$monthly\ range = N_{(\max)} - N_{(\min)} \quad (4)$$

Where,

N_{max} = Maximum daily radio refractivity within the month (N-units) and N_{min} = Minimum daily radio refractivity within the month (N-units).

The monthly refractivity range was then used to estimate the Field Strength Variability (FSV) as in Tanko *et al*, (2022).

$$FSV = (N_{(\max)} - N_{(\min)}) \times 0.2dB \quad (5)$$

Where, (FSV) is expressed in decibels (dB). The factor of 0.2 dB represents the empirical relationship adopted for frequencies within the 30–300 MHz band, whereby a unit change in surface radio refractivity corresponds to an approximate 0.2 dB change in field strength (Tanko *et al.*, 2025 and Adediji *et al.*, 2014).

Nonlinear Analysis

Nonlinear analysis was employed to investigate the temporal dynamics, persistence and predictability of field strength variability (FSV). Unlike conventional statistical techniques, nonlinear methods are capable of revealing hidden structures, deterministic patterns, and chaotic behaviour in atmospheric time series. In this study, three complementary nonlinear techniques were adopted: Hurst Exponent (HE) and Lyapunov Exponent (LE). These methods were used to characterize the dynamical behaviour of FSV, evaluate their long term memory characteristics and assess their predictability under different climatic conditions.

Hurst Exponent (HE)

The Hurst Exponent (HE) was employed to investigate the long term dependence, persistence/anti-persistence and memory characteristics of the FSV time series. The analysis was based on the rescaled range (R/S) approach, which evaluates the relationship between the range of cumulative

deviations and the standard deviation of a time series over different time scales (Hurst, 1951; Mandelbrot *et al.,* 1969).
Prior to the Hurst analysis, the time series was rescaled using the rescaledata function. The Hurst analysis was then performed using the MATLAB hurst function. A time series divisor of (d=10) was specified in the analysis. The function produced the Hurst related estimates as; H_{AL}, H_E and H_T, together with the 95% significance level p_{95}. In addition, the rescaled-range Hurst estimate H_{RS} was obtained using the RS1 function. The H_{RS} is the estimated Hurst exponent value in this research.

Lyapunov Exponent (LE)

The normalized time series was reconstructed in phase space using the time delay and embedding dimension obtained from the MATLAB phaseSpaceReconstruction function. The largest Lyapunov exponent was then estimated using lyapunovExponent, with a sampling frequency of (fs=1) and an expansion range of 200 (saturation range) $X_{min} = 2$ and $X_{max} = 200$. The largest Lyapunov exponent was calculated using (τ = 4), (m=10).

RESULTS AND DISCUSSION

Spatial Variation of FSV and Nonlinear Characteristics across the Climatic Regions

The results of the FSV, Hurst exponent (HE), and Lyapunov exponent (LE) analyses for the nineteen selected locations are presented in Table 1. The results reveal distinct spatial variations in both the magnitude and nonlinear characteristics of FSV across the climatic regions of Nigeria. The average FSV generally decreased from the northern dry regions towards the humid southern regions, while the sign and magnitude of the Lyapunov exponent also showed a clear regional pattern.

Figure 1: Bar Chart of Average Values of FSV

Figure 1 presents the average Field Strength Variability (FSV) across the nineteen selected locations in Nigeria. The results show a clear spatial gradient, with higher FSV in the northern regions and lower values toward the southern and coastal regions. Sokoto recorded the highest FSV (8.821 dB), followed by Katsina (8.562 dB), Yobe (8.397 dB), Kano (8.364 dB), and Borno (8.204 dB). The higher values in the northern regions may be associated with the predominantly dry conditions and lower atmospheric moisture, which can increase variations in radio refractivity and field strength (Tanko *et al.,* 2025; Ibrahim *et al.,* 2024).
The central locations recorded moderate FSV values, with Taraba having the highest value (7.899 dB), followed by Plateau (7.383 dB), Niger and Benue (6.969 dB), and FCT (6.913 dB). In contrast, the lowest FSV values were observed mainly in the Rainforest and Coastal regions. Edo, Ekiti, Anambra, Ebonyi, and Enugu recorded 4.765, 5.542, 5.114, 5.268, and 5.294 dB, respectively, while Lagos, Akwa Ibom, Rivers, and Bayelsa recorded 4.291, 4.532, 4.271, and 4.171 dB, respectively. Similar spatial and seasonal variations in radio propagation parameters have been reported across different climatic regions of Nigeria (Abimbola *et al.,* 2021; Bello *et al.,* 2025).
Overall, FSV generally decreases from the drier northern regions toward the more humid southern and coastal regions. This pattern reflects the strong climatic gradient across Nigeria and highlights the importance of atmospheric conditions in communication-system planning and radio link reliability.

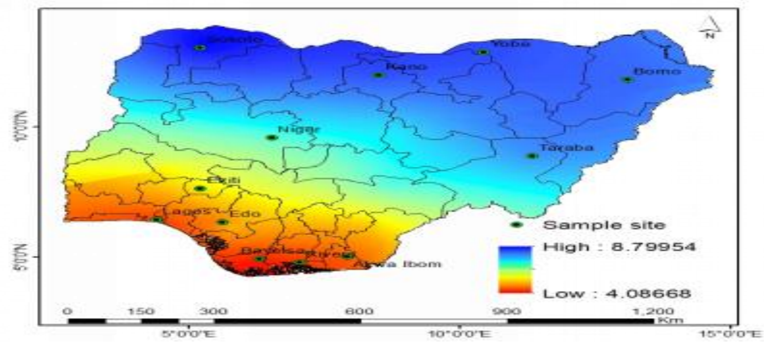

Figure 2: Spatial Map of Average Values of FSV

Figure 2 shows a clear south to north gradient in FSV, with higher values concentrated in the Sahelian and Sudan regions and progressively lower values toward the Guinea Savannah and Rainforest/Coastal regions. The Guinea Savannah exhibits intermediate FSV values, reflecting its transitional climatic conditions. The higher FSV in the northern regions may be associated with lower atmospheric moisture and humidity, whereas the lower values in the southern and coastal regions are consistent with their more humid conditions (Tanko *et al.,* 2025; Ibrahim *et al.,* 2024; Bello *et al.,* 2025). This spatial pattern highlights the influence of climatic and atmospheric conditions on FSV across Nigeria.

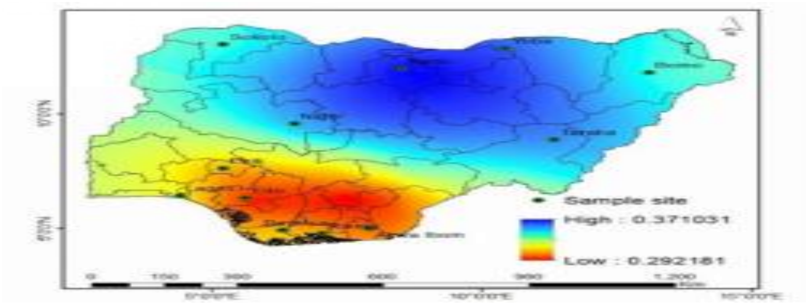

Figure 3: Spatial map of FSV HE

Figure 3 shows a general south to north increase in the Hurst Exponent (HE). However, all HE values are below 0.5, indicating predominantly anti-persistent FSV behaviour, whereby an increase is more likely to be followed by a decrease and vice versa (Sánchez-Granero *et al.,* 2008). This suggests that the FSV series exhibit weak long term persistence across all the study locations.

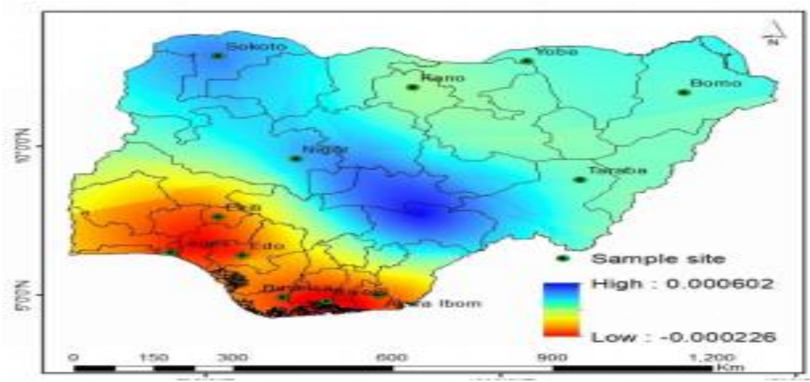

Figure 4: Spatial map of FSV LE

Figure 4 presents the spatial distribution of the Lyapunov Exponent (LE). Positive LE values observed in Sokoto, Yobe, Niger, and Taraba indicate sensitivity to initial conditions and unstable or chaotic dynamics, whereas the negative LE values observed from Edo to Bayelsa indicate more stable dynamics. The use of Lyapunov exponents to characterize atmospheric instability and predictability has also been reported in recent studies (Zhang *et al.,* 2024; Xavier *et al.,* 2024). Overall, the results indicate greater dynamical instability in the locations with positive LE values, while the negative LE values in the Rainforest/Coastal locations suggest comparatively more stable behaviour.

Overall, the combined spatial behaviour of FSV, HE and LE demonstrates that both the magnitude and dynamical characteristics of FSV vary across Nigeria. This finding is consistent with recent Nigerian studies showing substantial spatial and seasonal differences in field strength and radio propagation conditions across different climatic regions (Tanko *et al.,* 2022; Ibrahim *et al.,* 2024; Alagbe *et al.,* 2025; Bello *et al.,* 2025). Consequently, communication systems operating in different climatic regions may experience different levels of propagation variability and dynamical behaviour. Regional propagation models and link-planning strategies should therefore consider climatic differences rather than rely on a single nationwide characterization of FSV.

CONCLUSION

This study investigated the dynamical characteristics and spatial distribution of Field Strength Variability (FSV) across nineteen locations representing the major climatic regions of Nigeria using a nonlinear approach based on the Hurst and Lyapunov Exponents. The spatial analysis revealed a clear north to south distribution, with the regional mean FSV decreasing from 8.47 dB in the Sudan/Sahel region to 7.23 dB in the Guinea Savanna and 4.81 dB in the Rainforest/Coastal region, demonstrating the strong influence of climatic conditions on signal variability. The nonlinear dynamical analysis showed that the Hurst Exponent ranged from 0.2544 to 0.3850, with all values below 0.5, indicating predominantly anti-persistent FSV behaviour. The Lyapunov Exponent further revealed distinct regional dynamics, with positive values in the Sudan/Sahel and Guinea Savanna regions indicating sensitive dependence on initial conditions and chaotic behaviour, while predominantly negative values in the Rainforest/Coastal region suggested relatively more stable dynamics. Overall, the results demonstrate that both the magnitude and dynamical behaviour of FSV vary significantly across Nigeria and are strongly influenced by spatial and climatic conditions. These findings provide valuable information for radio propagation assessment and communication planning, particularly for the development of region specific strategies and propagation models capable of improving communication link reliability under varying atmospheric conditions. Although the study was limited by the use of reanalysis data and selected locations, future studies incorporating additional locations, higher resolution atmospheric datasets and long term ground based field strength measurements would improve the spatial representation and validation of FSV dynamics across Nigeria.

REFERENCES

Abimbola, O. J., Bada, S. O., Folaiye A. O., Suam, Y. M., Otto, M. S and Muhammad, S (2021). Estimation of Radio Refractivity from Satellite Derived Meteorological Data over a Decade for West Africa. *Scientific African Journal.* Pg14. https://doi.org/10.1016/j.sciaf.2021.e01054

Adediji, A. T., & Ajewole, M. O. (2008). Microwave propagation studies and fading phenomena over a tropical station. *Progress in Electromagnetics Research C, 5*, 71–84.

Ajayi, G. O., & Ofoche, E. B. (1984). Diurnal and seasonal variations of surface refractivity in Nigeria. *Journal of Atmospheric and Terrestrial Physics, 46*(6–7), 463–470.

Akpootu, D. O., Aminu, Z., Yusuf, A., Nouhou, I., Kola, T. A., Agidi, O. E., Salifu, S. I., Idris, M., Aliyu, M. A., & Aruna, S. (2024). Investigation of tropospheric radio refractivity and other relevant parameters using meteorological variables over Bauchi, Nigeria. *FUDMA Journal of Sciences*, *8*(2), 306–314. https://doi.org/10.33003/fjs-2024-0802-2366.

Alagbe, G. A. (2025). Investigation of diurnal and seasonal variation of radio refractivity and field strength over Ogbomoso, South Western Nigeria. In Proceedings of the 8th URSI-NG Annual Conference (URSI-NG 2024), *Advances in Physics Research.* https://doi.org/10.2991/978-94-6463-644-4_7

Ashidi, A. G. (2024). Autoregressive modelling of tropospheric radio refractivity over selected locations in tropical Nigeria using artificial neural network. Earth Science Informatics, Vol 17, page 5913–5922. https://doi.org/10.1007/s12145-024-01489-y.

Bello, G., Akpootu, D. O., Muhammad, J., Na-Allah, M., Balarabe, M., Babagana, A., & Idris, M. (2025). Investigation of field strength variability at ultra-high frequency and maximum angle of incidence in the Guinea and Coastal regions of Nigeria. *Saudi Journal of Engineering and Technology*, *10*(10), 522–530. https://doi.org/10.36348/sjet.2025.v10i10.004

Bichi, J. A., Tijjani, B. I., & Tikyaa, E. V. (2026). Analysis of spatial and temporal variation of deterministic chaos in tropospheric radio refractivity across twelve locations in Nigeria using recurrence quantification analysis. *Theoretical and Applied Climatology*, *157*, 360. https://doi.org/10.1007/s00704-026-06281-0

Echi, P. C., Udo, S. O., & Ewetumo, T. M. (2015). Chaotic behaviour of daily rainfall and temperature in Makurdi, Nigeria. *Theoretical and Applied Climatology, 121*(3–4), 581–589.

Fawupe, J. A., Ojo, S. O., & Olusola, J. O. (2016). Spatial analysis of deterministic chaos in rainfall and temperature over Nigeria. *Atmospheric Research, 182*, 135–145.

Gelaro, R., McCarty, W., Suárez, M. J., Todling, R., Molod, A., Takacs, L., Randles, C. A., Darmenov, A., Bosilovich, M. G., Reichle, R., Wargan, K., Coy, L., Cullather, R., Draper, C., Akella, S., Buchard, V., Conaty, A., da Silva, A. M., Gu, W., Zhao, B. (2017). The Modern-Era Retrospective Analysis for Research and Applications, Version 2 (MERRA-2). *Journal of Climate,* Vol 30(14), page 5419–5454. https://doi.org/10.1175/JCLI-D-16-0758.1

Hurst, H. E. (1951). Long-term storage capacity of reservoirs. *Transactions of the American Society of Civil Engineers, 116*, 770–799.

Ibrahim, U., Bawa, M., & Lawal, M. (2024). Estimating the variability of tropospheric radio refractivity and field strength over Enugu, South-East Nigeria. *International Journal of Science for Global Sustainability*, *10*(2), 251–257. https://doi.org/10.57233/ijsgs.v10i2.678

International Telecommunication Union. (2019). *The radio refractive index: Its formula and refractivity data* (Recommendation ITU-R P.453-14). ITU.

ITU-R. (2023). Recommendation P.453-15. The radio refractive index: Its formula and refractivity data. International Telecommunication Union, Geneva.

Kantelhardt, J. W., Koscielny-Bunde, E., Rego, H. H. A., Havlin, S., & Bunde, A. (2002). Detecting long-range correlations with detrended fluctuation analysis. *Physica A: Statistical Mechanics and its Applications, 295*(3–4), 441–454.

National Aeronautics and Space Administration (NASA). (2024). MERRA-2 data products. NASA Global Modeling and Assimilation Office (GMAO). Retrieved from https://gmao.gsfc.nasa.gov/reanalysis/MERRA-2/

Odafe Akpootu, D., Bello, G., Garba, I. I., Na-Allah, M., Muhammad, J., Balarabe, M., Aina, A. O., & Babagana, A. (2025). Analysis of field strength variability at ultra-high frequency and maximum angle of incidence across the Sahelian and Midland regions of Nigeria. *Arid-zone Journal of Basic & Applied Research*. https://doi.org/10.55639/607.02010071

Rasoul, A., Modarres, R., & Eslamian, S. (2014). Nonlinear dynamics and chaotic behaviour of rainfall in Ramsar, Iran. *Hydrological Sciences Journal, 59*(8), 1512–1523.

Rosenstein, M. T., Collins, J. J., & De Luca, C. J. (1993). A practical method for calculating largest Lyapunov exponents from small data sets. *Physica D: Nonlinear Phenomena, 65*(1–2), 117–134.

Sánchez-Granero, M. A., Trinidad Segovia, J. E., & García Pérez, J. (2008). Some comments on Hurst exponent and the long memory processes on capital markets. *Physica A: Statistical Mechanics and its Applications,* Vol.387 (22), 5543–5551. https://doi.org/10.1016/j.physa.2008.05.053.

Sánchez-Granero, M. A., Trinidad Segovia, J. E., & García Pérez, J. (2008). Some comments on Hurst exponent and the long memory processes on capital markets. *Physica A: Statistical Mechanics and its Applications, 387*(21), 5543–5551.

Tanko M, Akinbola A, M S Liman, J S Ojo. (2018). Assessment Tropospheric Variation of Radio Refractivity and Field Strength Variability over Some Selected Stations in Northern Nigeria. *Physical Science International Journal Vol*, 18(1); page 1-19. Article no. PSIJ.41320. ISSN: 2348-0130. DOI: https://doi.org/10.9734/PSIJ//2018/41320.

Tanko M, M. U. Sarki, U. Rilwan and I. S. Adeshina (2025). Tropospheric Radio Refractivity Mapping of Nigeria from satellite Data. *Nexus of Advanced Environmental Research.* 1(2025) pg 1-9. https://noaerjournal.com.

Tanko, M. M., Liman, M. S., Lumbi, W. L., Aliyu, U. S., & Sarki, M. U. (2022). Field strength variability mapping of Nigeria. *Journal of the Nigerian Society of Physical Sciences, 4*(3), 746. https://doi.org/10.46481/jnsps.2022.746

Tanko, M. M., Sarki, M.U and Bilya, M.A (2019). Seasonal Variation of Radio Refractivity of Some Selected Stations in Northern Nigeria. *Current Journal of Applied Science and Technology*. Vol. 32(1): page 1-12. https://doi.org/10.9734/cjast/2019/45326.

Tanko, M., Akinbobola, A., Liman, M. S., & Ojo, J. S. (2018). Assessment of tropospheric variation of radio refractivity and field strength variability over some selected stations in Northern Nigeria. *Physical Science International Journal, 18*(1), 1–19. https://doi.org/10.9734/PSIJ/2018/41320

Wolf, A., Swift, J. B., Swinney, H. L., & Vastano, J. A. (1985). Determining Lyapunov exponents from a time series. *Physica D: Nonlinear Phenomena, 16*(3), 285–317. https://doi.org/10.1016/0167-2789(85)90011-9

Xavier, A. K., Demaeyer, J., & Vannitsem, S. (2024). Variability and predictability of a reduced-order land–atmosphere coupled model. Earth System Dynamics, 15, 893–912. https://doi.org/10.5194/esd-15-893-2024

Zhang, M., Ding, R., Zhong, Q., Li, J., & Lu, D. (2024). Application of the conditional nonlinear local Lyapunov exponent to second-kind predictability. Advances in Atmospheric Sciences, 41(9), 1769–1786. https://doi.org/10.1007/s00376-024-3297-5